Lawson, M. T., K. K. Fuell, 2019: Gulf of Alaska cyclone in daytime microphysics RGB imagery. *J. Operational Meteor.*, **7** (3), 40-45, doi: https://doi.org/10.15191/nwajom.2019.0703

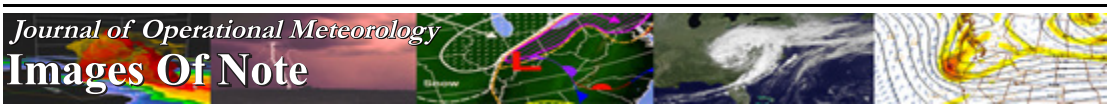

Gulf of Alaska Cyclone in Daytime Microphysics RGB Imagery

MICHAEL T. LAWSON
NOAA/National Weather Service, Anchorage, Alaska

KEVIN K. FUELL
University of Alabama Huntsville at NASA/SPoRT, Huntsville, Alabama

(Manuscript received 3 January 2019; review completed 11 March 2019)

1. Introduction

The NASA Short-term Prediction Research and Transition (SPoRT) Center has provided National Weather Service (NWS) Alaska Region forecasters with the experimental Daytime Microphysics (DtMicro) red-green-blue (RGB) product to support forecasting aviation hazards (Berndt et al. 2017), which has become an integral tool in the forecast process. On 11 March 2018, a rapidly deepening cyclone entered the Gulf of Alaska and developed gale-force winds and relatively strong convection for late winter, while low-level clouds and fog remained in its wake. The multi-spectral DtMicro RGB (Rosenfeld and Lensky 1998; EUMETSAT User Service Division 2009) provided an efficient product to analyze cloud properties and surface features with improved efficiency compared to single-channel visible or infrared imagery.

The DtMicro RGB and 0.64 µm visible images (Fig. 1) show a mature, occluded cyclone over the Gulf of Alaska at 2030 UTC (1230 LST). The DtMicro RGB combines visible and infrared channels related to cloud brightness, particle size, and temperature in order to analyze convective clouds and other cloud and surface features (Table 1; Lensky and Rosenfeld 2008). A limb correction and intercalibration was applied to infrared channels using the technique outlined in Elmer et al. (2016). These adjustments allow for greater consistency across the imager swath and consistency between numerous polar-orbiting satellites. The RGB clearly delineates the back-bent occlusion (dark orange to red), and dry air wrapping into the system, allowing a view of the low to mid-level clouds in the center of the image. Bright orange/yellow combinations over the Alaska panhandle and northwestern Canada are mountain-wave cirrus clouds composed of small ice particles. The magenta cloud features within the dry slot are deeper convective cells, and cyan to yellow-green cloud features are low-level water clouds. Near Illiamna, the tan to dull green coloring indicates very low stratus and fog, which is not distinguishable from snow cover in the visible imagery.

2. Discussion

The focus of this Image of Note will be on the convective snow showers (moderate orange- to red-colored cloud tops) located within the dry slot of the mature system (Figs. 1 and 2). Deep convection is a somewhat rare event in Southcentral Alaska, even in summer months let alone late winter. The cold air advection wrapping into the storm creates a favorable environment for convection as the maritime, arctic air interacts with the ice-free waters of the Gulf of Alaska, creating steep temperature lapse rates off the surface. The dry slot, coincident with cold advection, also steepens theta-e lapse rates from the surface through the low- to midlevels of the atmosphere. RGB imagery helps forecasters quickly identify these significant meteorological features, aiding in efficient situational awareness, thereby increasing the ability to issue forecasts in a timely manner. Although the visible channel (Fig. 1) does show high reflectance associated with the very thick cloud tops within the dry slot, the stronger convective elements stand out in the RGB (reds and dark oranges) against the midlevel clouds

Corresponding author address: Michael Lawson, 6930 Sand Lake Rd., Anchorage, AK 99502
E-mail: michael.lawson@noaa.gov

(magentas to pastel reds) that have large water droplets. The convective elements are also distinguishable from the low-level clouds (cyan to yellow-greens) that are composed of small to moderate water droplets (Fig. 1).

The DtMicro RGB creates an easily identifiable contrast between the deep-layer frontal clouds and cold advection behind the frontal occlusions, in addition to highlighting the convection within the dry slot. While the multi-channel RGB image does not explicitly sample instability, it can be inferred by the cellular nature of convective clouds within the dry slot (red to orange coloring). Large ice particles at the tops of towering clouds indicate strong convection, and small ice particles at similar cloud tops suggest severe convective updrafts where particles have quickly reached the cloud top before growing to a large size (Rosenfeld and Gutman 1994; Rosenfeld and Lensky 1998). Sampling the RGB color intensity values for the red/orange convective cells indicates a relatively low to moderate contribution of the green channel (i.e., large- to medium-size particles, Table 1) and a low contribution of the blue channel (i.e., cold temperatures). At the same time, a very large contribution is occurring in the red channel (i.e., very high reflectance due to ice). Other low- to mid-cloud objects in this region have a magenta coloring because of similar low green contributions in the convective cells, but fewer red and increased blue contributions (i.e., less reflectance and warmer). These magenta objects correspond to large water particles at lower heights and, therefore, weaker convection compared to the orange to red cloud objects, as confirmed by the Middleton Island, Alaska radar (PAIH) (Fig. 2). Note that the convective cells within the 10.8 μm single-channel imagery (Fig. 2) have a similar appearance to other cold clouds, but the DtMicro RGB adds cloud particle information to

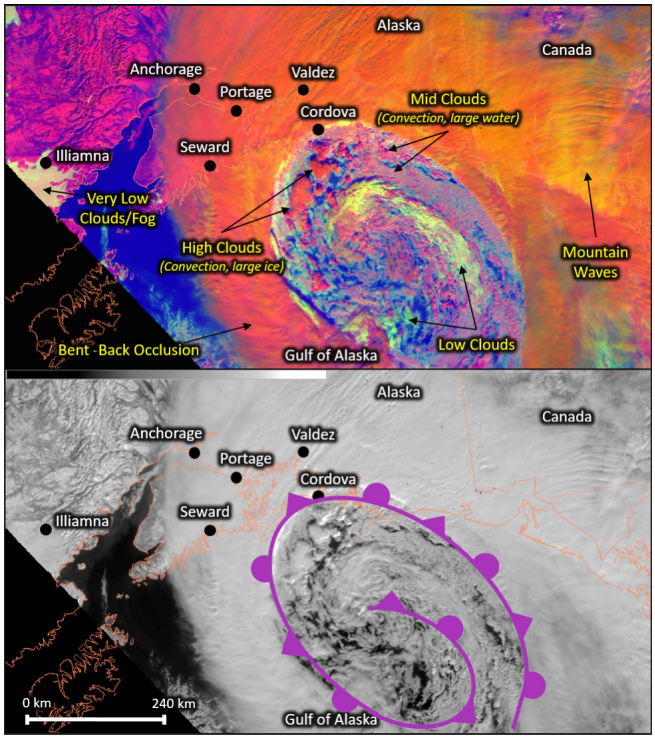

Figure 1. Daytime Microphysics RGB (upper panel) and 0.64 μm visible imagery (lower panel) at 2029 UTC 11 March 2018 from S-NPP Visible Infrared Imaging Radiometer Suite (VIIRS) imager. Visible imagery is provided for comparison to what forecasters typically use for daytime imagery and includes an annotation for the occluded front in purple. Although the frontal boundary is identifiable in both, other more subtle features noted in the RGB have less contrast in the visible image. *Click image for an external version; this applies to all figures hereafter.*

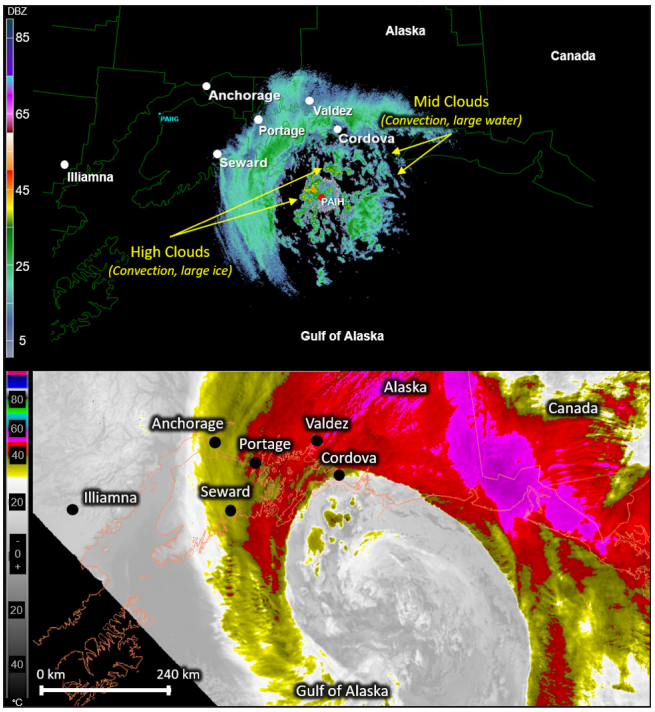

Figure 2. Radar reflectivity (DBZ) for the 0.5° elevation angle from Middleton Island, AK (PAIH) (upper panel) and longwave infrared 10.8 μm (°C) (lower panel) from S-NPP VIIRS imager for the same time as Fig. 1. Annotations of "High" and "Mid" clouds from the RGB portion of Fig. 1 are repeated on the upper panel for comparison of cloud features to reflectivity. The lower panel demonstrates traditional imagery used in operations and the lack of variation seen in the dry slot compared to the RGB image, as well as the inability to detect low stratus against the cold, underlying surface.

Table 1. Daytime Microphysics RGB color components and the associated Suomi National Polar-orbiting Partnership (S-NPP) VIIRS channels used. Other imagers may have slightly different center-channel values, but the same physical relationships and color contribution interpretation apply. "Small contribution to pixel" means that the value on a scale of 0–255 (i.e., byte value) is low, and the color component intensity is low (i.e., dark). "Large contribution to pixel" has a high byte value, and the color component intensity is bright. All three color components are combined for the resulting color at a pixel in the image. Note: The focus of the contribution interpretation is for cloudy areas. RGB colors in clear-sky areas will vary depending on the surface type and its associated spectral response per band.

Color Component	Band / Band Diff. (μm)	Physically relates to…	Small contribution to pixel indicates…	Large contribution to pixel indicates…
Red	0.87	Visible brightness of cloud as proxy to thickness	Thin cloud or non-reflective surface	Thick cloud (water and/or ice) or reflective surface
Green	3.7 (reflectance only)	Phase and particle size of cloud tops	Large particles in the cloud tops or on ground	Small water or ice particles in the cloud tops
Blue	10.8	Temperature of the surface being observed	Very cold clouds or surface	Very warm clouds or surface

Table 2. Surface METAR observations from Seward Airport (PAWD) from 2149 to 2353 UTC 11 March 2018. A short period of low-IFR visibility ensued. PAWD lies in a fjord that is not on the upslope side of the terrain for this flow pattern, so no orographic lift aids precipitation. Note that cloud level is in ft AGL, and visibility is in statute miles. [Not all METAR and SPECI (special, non-routine METAR) observations are included for brevity.]

Seward (PAWD)	Cloud (coverage and base level in hundreds of ft)	Visibility (statue miles)	Present Weather
2149 UTC 11 March 2018	BKN028 OVC036	4.00 sm	-SN
2153 UTC 11 March 2018	BKN028 OVC036	4.00 sm	UP
2201 UTC 11 March 2018	OVC024	3.00 sm	-SN
2206 UTC 11 March 2018	OVC022	1.75 sm	-SN
2214 UTC 11 March 2018	VV019	0.75 sm	-SN
2253 UTC 11 March 2018	VV018	0.75 sm	-SN
2306 UTC 11 March 2018	BKN020 OVC028	1.25 sm	-SN
2318 UTC 11 March 2018	BKN024 BKN031	3.00 sm	-SN BR
2322 UTC 11 March 2018	SCT026 BKN031	2.50 sm	UP
2338 UTC 11 March 2018	FEW033 BKN048	4.00 sm	UP
2353 UTC 11 March 2018	BKN055 BKN023	3.00 sm	UP

allow users to efficiently analyze strong versus weak convective clouds.

Verification of upstream, strong convection allowed higher confidence and detail in the Terminal Aerodrome Forecast (TAF) for Valdez (PAVD) and Cordova (PACV), including predominant and temporary groups of low Instrument Flight Rules (IFR) ceilings and visibility. Within two hours of the RGB image in Fig. 1, moderate to heavy snow was reported at a number of sites along the northern Gulf Coast of Alaska (Tables 2 and 3). Portage (PATO), Alaska, lies along the Seward Highway, which is the main (and only) artery between Anchorage and the Kenai Peninsula. Meteorological Aerodrome Report (METAR) observations highlighted the convective nature of the snow, particularly at Portage, where ceilings and vertical visibility quickly

Table 3. Surface METAR observations from Portage, AK (PATO) from 2144 to 0427 UTC for 11–12 March 2018. Note that cloud level is in ft AGL, and visibility is in statute miles. (Not all METAR and SPECI observations are included for brevity.)

Portage (PATO)	Cloud (coverage and base level in hundreds of ft)	Visibility (statue miles)	Present Weather
2144 UTC 11 March 2018	OVC021	1.25 sm	-SN BR
2153 UTC 11 March 2018	VV016	0.75 sm	-SN BR
2202 UTC 11 March 2018	VV011	0.50 sm	SN FG
2207 UTC 11 March 2018	VV009	0.25 sm	+SN FG
2300 UTC 11 March 2018	BKN023 OVC040	1.25 sm	-SN BR
2333 UTC 11 March 2018	VV012	0.25 sm	+SN FG
0000 UTC 12 March 2018	VV015	1.00 sm	-SN BR
0023 UTC 12 March 2018	VV011	0.25 sm	+SN FG
0041 UTC 12 March 2018	VV009	0.50 sm	SN FG
0125 UTC 12 March 2018	VV010	0.50 sm	-SN FG
0140 UTC 12 March 2018	VV009	0.25 sm	SN FG
0206 UTC 12 March 2018	VV010	0.50 sm	-SN FG
0226 UTC 12 March 2018	VV010	0.25 sm	+SN FG
0240 UTC 12 March 2018	VV010	0.50 sm	-SN FG
0353 UTC 12 March 2018	VV013	0.50 sm	SN FG
0427 UTC 12 March 2018	VV012	1.00 sm	-SN BR

dropped below 305 m (1000 ft), while visibility ranged from 0.4 km (0.25 sm) in heavy snow to 2 km (1.25 sm) in light snow over very short periods.

3. Summary

For the events of 11 March 2018, the DtMicro RGB provided operational value especially in enhancing situational awareness of convective snow and aviation hazards, providing confidence for decision making. Specifically, the RGB imagery aided forecasters in the following ways:

- The location of greatest instability in the dry slot was identified via the RGB cloud signatures in order to anticipate TAF site impacts of low ceilings and visibility.
- The RGB allowed multiple characteristics within a single product as opposed to using three different displays of single-channel imagery, making image analysis fast and efficient.
- The following synoptic and mesoscale features were easily identified: clear sky/snow cover, stratus/fog, convection, mid-level clouds, deep moisture, and mountain wave clouds.

RGB imagery on GOES-16/-17, Himiwari-8, and NOAA-20 is becoming more widely available and will add value beyond legacy single-channel imagery.

Acknowledgments: The Daytime Microphysics RGB is made available to NWS Alaska Region forecasters through a collaborative effort between the NASA SPoRT Center, the Geographic Information Network of Alaska (GINA), and NWS Alaska Region Headquarters. The S-NPP VIIRS data presented here were provided to the NWS offices by GINA direct broadcast capabilities, and SPoRT provided the Advanced Weather Interactive Processing System (AWIPS) configurations to display the RGB in the AWIPS. These activities were funded by Dr. Mitch Goldberg through the JPSS Proving Ground and Risk Reduction Program. The authors would like to thank Dr. Emily Berndt of NASA/SPoRT and Eugene Petrescu of NWS Alaska Region for their contributions and review of this manuscript. In addition, the authors

would like to recognize Frank LaFontaine of NASA/SPoRT for reprocessing of S-NPP VIIRS data, as well as Dr. Christopher Schultz for reprocessing radar data that contributed to the figures herein.

REFERENCES

Berndt, E., A. Molthan, W. W. Vaughan, and K. Fuell, 2017: Transforming satellite data into weather forecasts, *Eos*, **98**, CrossRef.

Elmer, N. J., E. Berndt, and G. J. Jedlovec, 2016. Limb correction of MODIS and VIIRS infrared channels for the improved interpretation of RGB composites. *J. Atmos. Oceanic Technol*., **33**, 1073–1087, CrossRef.

EUMETSAT User Service Division, 2009: *Best practices for RGB compositing of multi-spectral imagery.* 8 pp. [Available online at oiswww.eumetsat.int/~idds/html/doc/best_practices.pdf.]

Lensky, I. M., and D. Rosenfeld, 2008: Clouds-Aerosols-Precipitation Satellite Analysis Tool (CAPSAT). *Atmos. Chem. Phys*., **8**, 6739–6753, CrossRef.

Rosenfeld, D., and G. Gutman, 1994: Retrieving microphysical properties near the tops of potential rain clouds by multispectral analysis of AVHRR data. *Atmos. Res*., **34**, 259–283, CrossRef.

____, and I. M. Lensky, 1998: Satellite-based insights into precipitation formation processes in continental and maritime convective clouds. *Bull. Am. Meteorol. Soc*., **79**, 2457–2476, CrossRef.